



THE UNIVERSITY *of* EDINBURGH

Edinburgh Research Explorer

## Time-lapse gravity surveying as a monitoring tool for CO<sub>2</sub> storage

### Citation for published version:

Wilkinson, M, Mouli-castillo, J, Morgan, P & Eid, R 2017, 'Time-lapse gravity surveying as a monitoring tool for CO<sub>2</sub> storage', *International Journal of Greenhouse Gas Control*, vol. 60, pp. 93–99.  
<https://doi.org/10.1016/j.ijggc.2017.03.006>

### Digital Object Identifier (DOI):

[10.1016/j.ijggc.2017.03.006](https://doi.org/10.1016/j.ijggc.2017.03.006)

### Link:

[Link to publication record in Edinburgh Research Explorer](#)

### Document Version:

Peer reviewed version

### Published In:

International Journal of Greenhouse Gas Control

### General rights

Copyright for the publications made accessible via the Edinburgh Research Explorer is retained by the author(s) and / or other copyright owners and it is a condition of accessing these publications that users recognise and abide by the legal requirements associated with these rights.

### Take down policy

The University of Edinburgh has made every reasonable effort to ensure that Edinburgh Research Explorer content complies with UK legislation. If you believe that the public display of this file breaches copyright please contact [openaccess@ed.ac.uk](mailto:openaccess@ed.ac.uk) providing details, and we will remove access to the work immediately and investigate your claim.



# Time-lapse gravity surveying as a monitoring tool for CO<sub>2</sub> storage

Wilkinson M<sup>a</sup>., Mouli-Castillo J.<sup>a</sup>, Morgan, P.<sup>a</sup>, Eid R.<sup>a</sup>.

<sup>a</sup>School of GeoSciences, Grant Institute, The King's Buildings, James Hutton Road,  
Edinburgh EH9 3FE

Corresponding author; Mark Wilkinson, mark.wilkinson@ed.ac.uk

## Abstract

Time-lapse gravity surveys are a potential low cost method for detecting CO<sub>2</sub> migration from a storage site, particularly where accumulation within an overlying aquifer is predicted. **The modelled storage system consists of a storage reservoir (1000m crestal depth) and an overlying aquifer at variable depths (50 – 750 m crest), within a simple dome structure. In leakage scenarios, these are connected by a single vertical permeable pathway.** CO<sub>2</sub> leakage was simulated using the Permedia® CO<sub>2</sub> simulator, and a gravity model calculated to compare a leakage and a non-leakage scenario. Time-lapse gravity surveys are likely to be able to detect CO<sub>2</sub> leakage with CO<sub>2</sub> accumulation within an aquifer to depths of at least 750 m, at least within an actively subsiding sedimentary basin where sandstones are expected to have high porosities at shallow burial depths. For a high relief structure in which the CO<sub>2</sub> accumulates, the change in gravity cannot be used to detect the location of the leakage pathway as the measured gravity anomaly is centred on the geological structure. The first detection of leakage is possible after 11 - 15 years of leakage, though a maximum of only c. 1 % of injected CO<sub>2</sub> will have leaked at this time.

Keywords: storage; monitoring; time-lapse; gravity; CO<sub>2</sub> leakage

## Highlights

Detection of a leak is possible for accumulation depths of at least 750 m

- 30 Where possible, CO<sub>2</sub> leakage is detected when a maximum of c. 1 % has escaped
- 31 The escaped CO<sub>2</sub> becomes detectable after 11 - 15 years of leakage
- 32 The gravity anomaly does not give information about the location of the leakage point
- 33 Accumulation depth is the most important factor in determining utility of the technique

## 1. Introduction

Monitoring of CO<sub>2</sub> storage sites has been identified as a crucial component of Carbon Capture and Storage (CCS), not least because it may have to be conducted for relatively long periods of time after the cessation of injection at relatively low cost (e.g. Chadwick et al. 2009). Time-lapse gravity surveys could offer a cheaper alternative to seismic surveys (e.g. Fabriol et al. 2011), should the technique prove able to detect CO<sub>2</sub> leaks from the storage complex or / and migration within it. Existing experience includes downhole gravity monitoring in the Cranfield test site, USA (Dodds et al., 2013; Hovorka et al., 2013); the calculation of in-situ CO<sub>2</sub> density at Sleipner using high-precision seafloor stations (Nooner et al., 2007; Alnes et al., 2011), and the assessment of the lateral extent of a CO<sub>2</sub> plume (Alnes et al. 2011; Arts et al. 2008). Other low-cost monitoring technologies being developed include electrical resistance tomography (Carrigan et al., 2013). The aim of this paper is to assess, using realistic geometries of leakage plumes, if time-lapse gravity surveying might be used to detect CO<sub>2</sub> leakage, and how much CO<sub>2</sub> will have leaked at the time of first probable detection. As gravity anomalies are heavily influenced by the distance between the object of interest and the monitoring station (Fabriol et al. 2011; Skeels 1947), it is to be expected that gravity surveys are unlikely to be efficient at detecting changes occurring at great depths. As an example, surface gravity was rejected as a monitoring technique at the Quest CCS Project, Canada, where the reservoir is at about 2 km depth (Bourne et al., 2014) but has been demonstrated as useful for hydrocarbon reservoirs at similar depths (e.g. Ferguson et al., 2007) and for more shallow reservoirs (e.g. Krahenbuhl et al., 2010). Gravity monitoring has been tested at a number of producing gas fields, and is considered to be most feasible for shallow reservoirs of considerable lateral extent, with high porosities and high net-to-gross ratios (Young and Lumley, 2015, and refs therein).

## 2. Methodology

### 2.1 Geological Storage Model

The distribution of injected CO<sub>2</sub> was modelled using a simple geological model (Table 1) executed in the Permedia® CO<sub>2</sub> Darcy-flow simulator. A 200 m thick storage reservoir (hereafter termed the 'reservoir') has a depth-to-crest of 1000m (Fig. 1) and is overlain by an impermeable primary seal. A sandstone aquifer (hereafter termed the 'aquifer') is located vertically above the primary seal and is 200m thick with crestal depths of 50, 250, 500 and

750m in different versions of the model – the models are named after this crestal depth. A secondary seal lies between the aquifer and the ground surface. The model is 2000 m long and 2000 m wide (Fig. 1). All geological bounding surfaces are domes with 200m of vertical relief centred on a vertical axis running through the geometrical centre of the model. The edges of the model are open to porefluid flow as the aim of the model is to investigate monitoring, and not pressure changes within the reservoir. The cell size within the reservoir and aquifer was 40 by 40 m horizontally by 10 m vertically. The leakage scenario models (Fig. 1) are identical except that a vertical conduit of sandstone links the reservoir and the overlying aquifer which creates a migration path for the CO<sub>2</sub> from the reservoir to the overlying aquifer. The conduit is a single cell which is 40 by 40 m horizontally; the vertical dimension varies according to the depth of the aquifer, from 50 to 750 m.

The reservoir and aquifer sandstones are homogeneous, with an exponential porosity-depth function giving an average porosity of the aquifer of c. 37 % at the shallowest depth modelled (50 m) ranging to c. 20 % for the most deeply buried reservoir (1500 – 1900 m depth). The base 10 logarithm of horizontal permeability is proportional to porosity, with a range of averages of 30 to 200 mD; vertical permeability is one tenth of horizontal permeability. Non-reservoir (seal) units are both porous and permeable, but are not penetrated by either free-phase or dissolved CO<sub>2</sub> during the simulations. Sandstone imbibition and drainage were modelled using relative permeability and capillary pressure curves from the Cardium Sandstone (Bennion & Bachu 2006). Modelled brine imbibition resulted in residual trapping of 20% of the CO<sub>2</sub> present in the pore space. The irreducible water saturation was 20%, although this value was never reached during simulations. CO<sub>2</sub> density was calculated from the Duan & Sun (2003) equation of state (Fig. 2). The temperature gradient was 30°C / km and the pressure gradient was 10MPa / km. An injection well is present diametrically opposite to the leak point, at 500 m from the model boundaries, with a 100 m perforated interval within the reservoir (Fig. 1). Simulations were run for each of the models with an injection rate of 1 Mt / year of CO<sub>2</sub> for 30 years, with an overall simulation period of 80 years. Data passed on to the subsequent gravity modelling contained, for each cell of the geological model, the spatial coordinates, the CO<sub>2</sub> saturation, the CO<sub>2</sub> density, the brine density, the grain density, the cell volume and the porosity.

## 2.2 Gravity Modelling

The modelled results of gravity surveys conducted at the horizontal ground surface (or sea bed) were calculated for both leakage and non-leakage models using the 'R' programming language. The surface gravity monitoring stations were placed along a line running diagonally across the model (Fig. 1) and hence passing above both the injection well and the

leakage pathway. The incremental gravitational attraction,  $Dg$ , between a given model cell and a given monitoring station was calculated from Equation 1:

$$Dg = \frac{G V_n \rho_n}{r_n^2} \quad (1)$$

where  $G$  is the universal gravitational constant;  $V_n$  is the volume of the  $n$ th cell;  $\rho_n$  is the bulk density of the cell; and  $r_n$  is the distance from the measuring station to the centre of the cell.

The bulk density of the cell ( $\rho_n$ ) is given by:

$$\rho_n = (1 - \phi_n) \times \rho_{grain_n} + \phi_n \times \left[ (1 - S_{CO_2n}) \times \rho_{brine_n} + S_{CO_2n} \times \rho_{CO_2n} \right] \quad (2)$$

where  $\phi_n$  is the porosity of the cell;  $\rho_{grain}$  is the grain density (a constant 2650 kg / m<sup>3</sup>);  $S_{CO_2}$  is the saturation of free-phase CO<sub>2</sub> in the porosity;  $\rho_{brine}$  is the density of the brine; and  $\rho_{CO_2}$  is the density of the CO<sub>2</sub>. The calculation was repeated for each cell in the model and the incremental values summed to provide the total gravitational attraction at each monitoring station. This process was done for each model in the pairs: the leakage and non-leakage scenarios for each time step. For the non-leakage scenarios, the calculated gravity values were then subtracted from the baseline (time zero) readings to obtain the total change in gravity measurements due to the injection of CO<sub>2</sub> into the reservoir. For the leakage scenarios, at each desired time step the calculated gravity for the leakage model was subtracted from the calculated gravity for the non-leakage model at the same time and for the same depth of aquifer. The reported gravity anomaly is hence the deviation from the expected (non-leakage) scenario.

The gravity model was tested against the results of Chadwick et al. (2009, their Fig. 4) and was able to reproduce the modelled gravity anomaly in both their no-leakage and leakage scenarios. A 5  $\mu$ Gal threshold value was chosen as the minimum difference between surveys likely to be detectable using current gravity meters, a value comparable to the repeatability calculated at Sleipner of 5.3  $\mu$ Gal (Nooner et al., 2007) and slightly greater than the 4.2  $\mu$ Gal average for gravity surveys completed between 2005 and 2007 at Norwegian offshore gas fields (Zumberge et al. 2008). A repeatability of 12  $\mu$ Gal standard deviation has been reported at Prudhoe Bay (Alaska) for surface-based GPS-controlled relative gravimeter surveys (Ferguson et al., 2007), suggesting that the 5  $\mu$ Gal resolution may be optimistic unless semi-permanent base-stations can be established.

### 3. Results

Figure 3 shows the variation in gravity anomaly for the 80 years of simulation for a no leakage scenario. The anomaly increases up to a maximum value of c. -25  $\mu\text{Gal}$  at the end of the 30 year injection phase (Table 2), with some asymmetry due to a slightly higher anomaly close to the injection point. After injection, the magnitude of the anomaly remains approximately constant, but becomes symmetrical as the  $\text{CO}_2$  settles into the trapping structure. Fig. 4 shows the difference in gravity measured at the surface between the leakage and non-leakage scenarios after 80 years of simulation for the 4 modelled aquifer geometries; and Fig. 5 shows the anomalies through the 80 years of simulation. The gravity anomaly is smaller when the aquifer is deeper, only c. 50  $\mu\text{Gal}$  for the 750 m deep aquifer compared to c. 970  $\mu\text{Gal}$  for the 50 m deep aquifer. The leaking  $\text{CO}_2$  is detectable at the surface only after 20 - 25 years after the start of injection, when 6 – 240 kt of  $\text{CO}_2$  have entered the aquifer due to 11 – 15 years of leakage, i.e. when less than 1 % of the  $\text{CO}_2$  injected at that time has leaked (Table 3). The gravity anomaly measured at the surface is centred on the crest of the aquifer structure at all times when it is above the assumed detection threshold, i.e. does not reveal the actual site of the leakage pathway.

### 4. Discussion

With a reasonably realistic, modelled, geometry of the leaking  $\text{CO}_2$  plume, assumed to be accumulating within an aquifer above the primary storage reservoir, then changes in gravity anomaly due to leakage are detectable using monitoring stations located at the ground surface or seabed, for all the scenarios modelled here i.e. with the aquifer 750m or less below the surface. In the absence of an aquifer in which the  $\text{CO}_2$  can accumulate, displacing a significant volume of more dense water in a relatively localised area, then detection of leakage could still occur, but the change of anomaly will be much smaller - the change in gravity due to the injection of 30 Mt of  $\text{CO}_2$  is at c. 1000m is c. 25  $\mu\text{Gal}$  (Table 2). With a 5  $\mu\text{Gal}$  detection limit, a loss of  $\text{CO}_2$  by leakage to the surface of c. 6 Mt should be detectable in theory. However, if the  $\text{CO}_2$  is trapped within an aquifer, as modelled here, then the limit of detection is much lower, from 0.03 Mt if the aquifer is at only 50 m depth (Table 3). The results are comparable but not identical to those of Chadwick et al. (2009)

who suggested if the CO<sub>2</sub> pooled at 500m depth then c. 1 Mt might be detectable, whereas here we predict, with a 500m deep aquifer, a detection limit of only 0.3 Mt (Table 3).

The larger (and hence more readily detectable) gravity anomalies at shallow depth are the result of 2 factors: the density of the CO<sub>2</sub> and the distance from the measuring stations. The lower pressures at depth result in a significant lowering of the density of the CO<sub>2</sub> to just less than 100 kg / m<sup>3</sup> in the most shallow parts of the aquifer compared to c. 800 kg / m<sup>3</sup> in the reservoir at 1000m (Fig. 2), so that the mass change caused by CO<sub>2</sub> displacing brine (of approximately constant density) is significantly greater at shallow depths. The density of the CO<sub>2</sub> is dependent upon both the surface temperature and the geothermal gradient, however the sensitivity of these input parameters was not tested in this study. Gravity effects also reduce as the square of the distance between two masses, so that a shallow aquifer, which is relatively close to the surface, will show a greater gravity anomaly for a given density change than a deeper one. The effect of the dissolution of the injected CO<sub>2</sub> into the porewater are two-fold. Firstly, there is a decrease in the total free-phase CO<sub>2</sub> compared to the volume injected (c. 30 % dissolved at 80 years), and secondly there is the formation of CO<sub>2</sub>-rich brine with a maximum density of 1072 kg / m<sup>3</sup> compared to an initial 1025 kg / m<sup>3</sup>. The relatively high density brine will reduce the net gravity anomaly detected at the surface, but evidently the effect is too small to mask the low density of the accumulated free phase CO<sub>2</sub>. There is little change in the proportion of dissolved CO<sub>2</sub> after the end of injection in the no-leak scenario (26.5 % at the end of injection at 30 years versus 30 % at 80 years) – the free-phase CO<sub>2</sub> remains stable, trapped within the dome of the reservoir, and the residual water directly in contact with the CO<sub>2</sub> is presumably saturated with CO<sub>2</sub> by 30 years. A small amount of CO<sub>2</sub>-saturated brine sinks from the CO<sub>2</sub>-water interface which presumably brings unsaturated water from below into contact with the CO<sub>2</sub> pool, but not sufficient to cause significant additional dissolution. The modelled dissolution rate (< 1 % per year) is comparable to the rate suggested by Alnes et al. (2011) based on the modelling of gravity data at the Sleipner injection site of a maximum of 1.8 % of total CO<sub>2</sub> per year.

The modelled square grid of gravity monitoring stations (2 by 2 km) is probably rather more extensive than might be deployed in a real-world situation, and for example differs from the ones utilised at Sleipner which consisted of two lines of monitoring stations perpendicular to one another, centred on the point of CO<sub>2</sub> injection (Arts et al. 2008; Alnes et al. 2011). Consequently rather less data would probably be available than is calculated here. However, the modelled anomalies are centred on the geological structure of the aquifer, and not the



leakage site. While this has the disadvantage that there is no information available about the site of the leakage, there is the advantage that the monitoring stations can be placed above the crest of the aquifer structure, hence maximising the probability of early detection. In plan view, the gravity anomalies are approximately circular, i.e. mirror the shape of the dome of the aquifer, and allow an estimate to be made of the lateral distance over which detection is possible, i.e. how close a linear monitoring array must be to the locus of leakage for successful detection. Depending upon the depth of the aquifer, an anomaly width of 400 m is achieved within 20 – 25 years, so that gravity measuring stations of a few hundred metres lateral separation should achieve detection at this stage. It is however clear that, if the CO<sub>2</sub> in the reservoir migrates laterally out with the monitored area before breaching the primary seal, or if the aquifer has a structure that directs buoyant migration of the CO<sub>2</sub> laterally away from the injection site, then the secondary CO<sub>2</sub> plume in the aquifer may go undetected.

The time at which first detection of the leak would occur also depends upon the depth of the aquifer (Table 3), with a pattern that is not just a greater elapsed time for deeper aquifers as might have been expected. It is probable that the control on the leakage rate was at least partly the length of the leakage column – which is shortest for the model with the deepest aquifer. Hence, the leakage pathway was shortest for the deepest aquifer. In addition, the leakage columns provided a pressure-valve effect. As more CO<sub>2</sub> was injected into the reservoir, the pressure within the reservoir increased, resulting in a greater pressure gradient between it and the aquifer. The leakage pathway also acted as a pressure release column through which fluid moved along this pressure gradient. In the models in which the leakage pathway was shorter, fluids moved more rapidly from the reservoir to the aquifer. This compensated for the higher mass of CO<sub>2</sub> required for detection in the models with a deeper aquifer, but only for a short period of time after first CO<sub>2</sub> migration. Figures 4 and 5 show that, after this initial time period, the larger anomalies are associated with the shallower aquifers. The time between surveys could also influence the time of first detection - the longer the intervals between individual surveys, then the more CO<sub>2</sub> may have leaked before detection. Permanent arrays of detectors on the sea bed are an option to enable the collection of high frequency data, but any such equipment would have to be **resistant to trawling**. Nooner et al. (2007) describe a ‘permanent’ concrete gravity station having been dragged for 20 m along the sea bed, presumably by a trawl net, which might result in expensive damage to any gravity meter left in-situ. Power must also be supplied to any such meters, and data collected, requiring repeated visits or a sub-sea cable and a nearby platform, any of which would increase costs substantially. In contrast, semi-permanent

concrete survey stations (as markers of survey locations) appear to be largely effective as a means of ensuring the repeatability of time-lapse measurements (Nooner et al., 2007).

Assuming that a leak of CO<sub>2</sub> is detected in a real storage site, then steps would presumably be taken to remediate the leak. Some remediation techniques such as a hydraulic barrier have been modelled at only 10 m lateral distance from a leak (Réveillère et al. 2012), which clearly requires high precision knowledge of the leak location in the subsurface. It is virtually impossible that gravity monitoring will provide such high spatial resolution, even under ideal conditions. It should be noted that modelling of leakage within very low-relief structures (not reported here) suggests that the initial CO<sub>2</sub> plume can be detected above the leakage site, before migration to any local structural high masks the signal. For remediation techniques such as water injection to increase residual saturation trapping, or the recovery of the leaked CO<sub>2</sub> through purpose-drilled wells (Manceau et al, 2014), then the gravity technique has the potential to provide the spatial location of the CO<sub>2</sub> with sufficient resolution.

CO<sub>2</sub> migration into the aquifer is a two stage process, of vertical migration followed by the formation of a so-called gravity tongue as the CO<sub>2</sub> spreads laterally below the overlying seal (e.g. Esposito and Benson, 2012). Detection of leakage before the CO<sub>2</sub> reaches the top of the aquifer is not possible for the aquifer geometries reported here, so that detection will only occur after sufficient CO<sub>2</sub> has accumulated in the aquifer to form a gravity tongue. **If a gravity tongue is not formed, i.e. if a thick and suitably placed aquifer is not present, then the possibility of detection of leakage by the gravity method must be substantially reduced, but is not modelled here.** There is a finite time between the onset of injection and a leak occurring, while the CO<sub>2</sub> migrates from the injection point to the leakage site. There is then a further time period before the leak becomes detectable, which is between 6 and 12 years (Table 3). However, the proportion of CO<sub>2</sub> leaked before first possible detection is low – less than or equal to 1 % of the total injected at the time of detection, with the lowest proportions leaked in the scenarios with the shallowest aquifers (Table 3).

#### **4.1 Comparison with case studies**

Gravity monitoring has been trialled at the Sleipner injection site with time-lapse seafloor gravity surveys carried out in 2002, 2005, 2009 and 2011 (Arts et al. 2008; Alnes et al. 2011; Noonan et al., 2007). Alnes et al. (2011) detected a -10 µGal gravity anomaly in 2002 from

5.2 Mt of CO<sub>2</sub> at c. 800 m depth, i.e. 2 µGal per Mt CO<sub>2</sub>. Here, for a non-leakage scenario comparable to the Sleipner case, we have a lower figure that varies from 0.8 to 1.5 µGal per Mt of total CO<sub>2</sub> injected, or 1.2 to 1.7 µGal / Mt of free-phase CO<sub>2</sub> (Table 2). The reservoir that is modelled here is a little deeper than the Sleipner one, which has a crest at c. 800 m (Zweigel et al., 2004), so that the CO<sub>2</sub> is at a greater distance from the surface. However the most important factor is probably the density of the CO<sub>2</sub>. Alnes et al. (2011) estimated the in-situ CO<sub>2</sub> density in Sleipner to be  $675 \pm 20$  kg / m<sup>3</sup> theoretically, or  $720 \pm 80$  kg/m<sup>3</sup> as a best estimate, where the modelling presented here produces a figure of 796 – 836 kg / m<sup>3</sup>. The water density is also important (as it is the density contrast between the CO<sub>2</sub> and the displaced water that is important, not either absolute density of either phase), unfortunately Alnes et al. (2011) do not give a value for this. Nooner et al. (2007), also reported gravity data from the Sleipner site but after the injection of 7.7 (2005) and 11 (2009) Mt of CO<sub>2</sub>. They calculated an in-situ CO<sub>2</sub> density of  $530 \pm 65$  kg/m<sup>3</sup> (95% confidence), again much lower than the value calculated here, resulting in higher changes per Mt of CO<sub>2</sub> than reported here. Based on these results, Jenkins et al. (2015) concluded that large stored amounts of CO<sub>2</sub> (>50 Mt) should be suitable for characterisation by gravimetric survey in many scenarios, but that offshore seabed gravimetry is expensive compared to the same technique conducted on land. The results of this paper show that gravimetric surveys can also be feasible for detecting small fractions of leakage, perhaps using the methodology of Krahenbuhl et al. (2010). The porosity of the sandstone hosting the CO<sub>2</sub> is also important, in that a high porosity sandstone has more water available for displacement by CO<sub>2</sub> than a lower porosity one. The porosity values modelled here at the depths of the Sleipner aquifer (c. 800 – 1000 m) are lower than that aquifer (18 – 23 % compared to 36 – 40 % porosity; Zweigel et al., 2004) which will reduce the calculated gravity anomaly in the model compared to the Sleipner case.

Although gravity surveying is commonly assumed to be useful only at shallow depths of burial (e.g. Chadwick et al., 2009), a study of water flooding in a Prudhoe Bay (Alaska) gas field predicted maximum gravity changes of 200 µGal despite a reservoir depth of 2500 m (Ferguson et al., 2007). Smaller ‘thief zone’ features of 10 – 20 µGal were also predicted, more comparable to the magnitude of gravity anomalies predicted here. Again, the density contrast of the 2 fluids is crucial in determining the usefulness of the gravity method, and the methane gas in the Prudhoe Bay field has a lower density than CO<sub>2</sub> under equivalent conditions, and hence a higher density contrast with water or brine.

## 4.2 Limitations of the model

The model has simple geology with no heterogeneity within either the reservoir or the aquifer. Given the depth of the reservoir, and the magnitude of the gravity anomalies associated with CO<sub>2</sub> injection in the non-leaking scenario, adding heterogeneity to the reservoir would most probably have no significant effect on the results. Heterogeneity in the aquifer might either reduce the CO<sub>2</sub> average saturation of CO<sub>2</sub> due to unfilled regions such as shales or siltstones, or locally increase it by focussing migration, for example within channel sandstones. The former scenario seems more probable, such that the results presented here should be regarded as best-case scenarios. The overall geometry of the model is also simple, though more realistic than that used by Chadwick et al. (2009) in their assessment of the feasibility of gravity monitoring for the detection of a CO<sub>2</sub> leak. Young and Lumley (2015) compared calculated gravity anomalies for a complex, realistic, geological model of a gas field against a simple geometrical model (in this case a vertical cylinder, their Table 3) and found that the discrepancy between the two models was  $\pm 6 \mu\text{Gal}$ . They concluded, for the case of the high density contrast between methane and water, that even a highly simplified geometry gave an estimate of gravity anomaly with first-order accuracy, but that for increased accuracy, especially for aspects such as the symmetry of an anomaly, then a more accurate model was required. In contrast, Krahenbuhl and Li (2012) report that the interpretation of gravity data for the change in fluids at reservoir depths requires complex model construction, beyond the complexity of the model presented here. However, they are considering only small density contrasts (e.g.  $60 \text{ kg / m}^3$ ) compared to a CO<sub>2</sub>-brine contrast, so that less complex models may suffice for at least the initial interpretation of CO<sub>2</sub> leakage. The model described here did not incorporate regional groundwater flow in the aquifer, which is perhaps realistic in an offshore setting but could be misleading in an active aquifer with topographically-driven flow of 10's m per year. This could rapidly move the CO<sub>2</sub> out of the monitored area, and would need to be considered in the design of a monitoring scheme.

The model assumes that the porosity of the sandstone within both the aquifer and the reservoir decrease with depth exponentially. This results in a high porosity for the most shallowly buried of the modelled aquifers, with an average porosity of approximately 37 % at the shallowest depth modelled (50 m). However, at the depths of the Sleipner aquifer (c. 800 – 1000 m), porosity values in the modelled aquifer are lower than the Sleipner aquifer (18 – 23 % compared to 36 – 40 % porosity; Zweigel et al., 2004) which will approximately halve

the expected gravity anomaly in the model compared to the Sleipner case. The modelled porosity – depth relationship is probably acceptable in a basin which is actively subsiding and in which sediment is actively accumulating, but it would be too high if the basin had been tectonically inverted, so that older, more consolidated (and lower porosity) sediments were close to the surface. While the modelled results are hence likely to be applicable to an offshore setting in an active basin such as the North Sea or USA Gulf Coast, the modelled gravity anomalies will be of lower amplitude on land or if uplifted sediments are close to the seabed, as there is less porewater within the porosity to replace with low density CO<sub>2</sub>. In this case, modelling with more appropriate porosities would be required. In the event that a gravity survey conducted at the surface cannot provide sufficient resolution, then measurements taken downhole can significantly improve the results, provided that suitable boreholes are in place (Krahenbuhl et al., 2015).

## 5. Conclusions

Modelling of time-lapse gravity surveys conducted at the sediment surface over a leaking CO<sub>2</sub> store, with CO<sub>2</sub> accumulation in a shallow overlying aquifer, suggests that the leakage can be detected when only a small quantity of CO<sub>2</sub> has escaped (< 1 % or better), at least in an offshore setting with high porosity sediments close to the surface. Detection is possible under favourable circumstances, to depths of at least 750m for the crest of the aquifer.

Assuming a 30 year injection phase, then detection should occur before the closure of the CO<sub>2</sub> injection site. The resulting gravity anomaly will not give information about the location of the leakage point for the high-relief structure modelled here.

The presence of an aquifer in which the CO<sub>2</sub> can accumulate is the most important factor in determining the sensitivity of the gravity monitoring technique. Without a shallow aquifer in which the CO<sub>2</sub> accumulates, a gravity anomaly due to leakage could be detected from the surface but would require a far larger leak than if the CO<sub>2</sub> can accumulate at an intermediate depth.

## Acknowledgements

368 Thank you to 2 anonymous reviewers, for suggesting significant improvements. The  
369 University of Edinburgh acknowledges support of this work by Halliburton Software and  
370 Services, a Halliburton Company.

## References

- Alnes, H., Eiken, O., Nooner, S., Sasagawa, G., Stenvold, T. & Zumberge, M., 2011. Results from Sleipner gravity monitoring: Updated density and temperature distribution of the CO<sub>2</sub> plume. *Energy Procedia*, 4, 5504–5511.
- Arts, R. et al., 2008. Ten years' experience of monitoring CO<sub>2</sub> injection in the Utsira Sand at Sleipner. *Offshore Norway. First Break*, 26, 65–72.
- Bennion, D.B. & Bachu, S., 2006. Dependence on temperature, pressure, and salinity of the IFT and relative permeability displacement characteristics of CO<sub>2</sub> injected in deep saline aquifers. *Society of Petroleum Engineers paper* 102138.
- Bourne, S., Crouch, S. & Smith, M., 2014. A risk-based framework for measurement, monitoring and verification of the Quest CCS Project, Alberta, Canada. *International Journal of Greenhouse Gas Control*, 26, 109–126.
- Carrigan, C.R., Yang, X., LaBrecque, D.J., Larsen, D., Freeman, D., Ramirez, A.L., Daily, W., Aines, R., Newmark, R., Friedmann, J. & Hovorka, S., 2013. Electrical resistance tomographic monitoring of CO<sub>2</sub> movement in deep geologic reservoirs, *International Journal of Greenhouse Gas Control*, 18, 401-408.
- Chadwick R.A. Arts, R., Benthams, M., Eiken, O., Holloway, S., Kirby, G. A., Pearce, J. M., Williamson, J. P., and Zweigel, P., 2009. Review of monitoring issues and technologies associated with the long-term underground storage of carbon dioxide. In: D. J. Evans and R. A. Chadwick, *Underground Gas Storage: Worldwide Experiences and Future Development in the UK and Europe*. Geological Society Special Publication 313, 257 – 275.

399 Dodds, K., Krahenbuhl, R., Reitz, A., Li, Y., & Hovorka, S., 2013. Evaluating time-lapse  
400 borehole gravity for CO<sub>2</sub> plume detection at SECARB Cranfield. *International Journal of*  
401 *Greenhouse Gas Control*, 18, 421-429.

402

403 Duan, Z. & Sun, R., 2003. An improved model calculating CO<sub>2</sub> solubility in pure water and  
404 aqueous NaCl solutions from 273 to 533 K and from 0 to 2000 bar. *Chemical Geology*, 193,  
405 257–271.

406

407 Esposito, A. and Benson, S.M., 2012. Evaluation and development of options for remediation  
408 of CO<sub>2</sub> leakage into groundwater aquifers from geologic carbon storage. *International Journal*  
409 *of Greenhouse Gas Control*, 7, 62 – 73.

410

411 Fabriol, H., Bitri, A., Bourgeois, B., Delatre, M., Girard, J.F., Pajot, G., Rohmer, J., 2011.  
412 Geophysical methods for CO<sub>2</sub> plume imaging: Comparison of performances. *Energy*  
413 *Procedia*, 4, pp.3604–3611.

414

415 Ferguson, J. F., Chen, T., Brady, J., Aiken, C. L. V. and Seibert, J. 2007. The 4D  
416 microgravity method for waterflood surveillance II — Gravity measurements for the Prudhoe  
417 Bay reservoir, Alaska. *Geophysics*, 72, I33–I43.

418

419 Hovorka, S.D., Meckel, T.A. & Treviño, R.H., 2013. Monitoring a large-volume injection at  
420 Cranfield, Mississippi—Project design and recommendations. *International Journal of*  
421 *Greenhouse Gas Control*, 18, 345-360.

422

423 Jenkins, C., Chadwick, A., Hovorka, S.D., 2015. The state of the art in monitoring and  
424 verification—Ten years on. *International Journal of Greenhouse Gas Control*, 40, 312–349.

425



Krahenbuhl, R.A. and Li, Y., 2012. Time-lapse gravity: A numerical demonstration using robust inversion and joint interpretation of 4D surface and borehole data. *Geophysics*, 77, G33–G43.

Krahenbuhl, R.A., Martinez, C., Li, Y. and Flanagan, G., 2015. Time-lapse monitoring of CO<sub>2</sub> sequestration: A site investigation through integration of reservoir properties, seismic imaging, and borehole and surface gravity data. *Geophysics*, 80, WA15–WA24.

Krahenbuhl, R.A. and Li, Y. and Davis, T., 2010. 4D gravity monitoring of fluid movement at Delhi Field, LA: A feasibility study with seismic and well data. SEG Denver 2010 Annual Meeting, p. 4210 – 4214. <https://www.onepetro.org/download/conference-paper/SEG-2010-4210?id=conference-paper%2FSEG-2010-4210>

Manceau J.-C., Hatzignatiou, D.G., de Lary, L., Jensen, N.B. Réveillère, A., 2014. Mitigation and remediation technologies and practices in case of undesired migration of CO<sub>2</sub> from a geological storage unit—Current status. *International Journal of Greenhouse Gas Control*, 22, 272 – 290.

Nooner, S.L., Eiken, O., Hermanrud, C., Sasagawa, G.S., Stenvold, T. & Zumberge, M.A., 2007. Constraints on the in situ density of CO<sub>2</sub> within the Utsira formation from time-lapse seafloor gravity measurements. *International Journal of Greenhouse Gas Control*, 1, 198–214.

Réveillère, A., Rohmer, J., and Manceau, J.-C., 2012. Hydraulic barrier design and applicability for managing the risk of CO<sub>2</sub> leakage from deep saline aquifers. *International Journal of Greenhouse Gas Control*, 9, 62 – 71.

Skeels, D.C., 1947. Ambiguity in Gravity Interpretation. *Geophysics*, 12, p.43–56.

455 Young, W.M. and Lumley, D., 2015. Feasibility analysis for time-lapse seafloor gravity  
456 monitoring of producing gas fields in the Northern Carnarvon Basin, offshore Australia.  
457 Geophysics, 80, p. WA149–WA160.

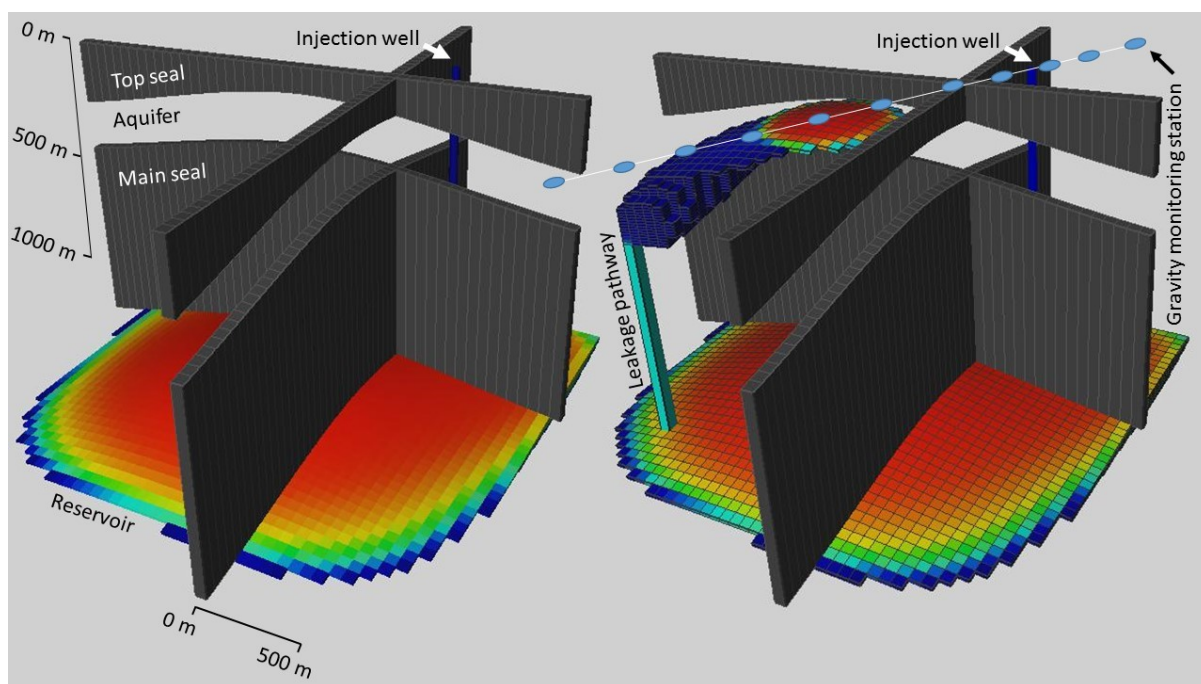
458

459 Zumberge, M. Alnes, H., Eiken, O., Sasagawa, G., and Stenvold, T., 2008. Precision of  
460 seafloor gravity and pressure measurements for reservoir monitoring. Geophysics, 73,  
461 WA133–WA141.

462

463 Zweigel, P., Arts, R. Lothe, A., and Lindeberg, E., 2004. Reservoir geology of the Utsira  
464 Formation at the first industrial scale underground CO<sub>2</sub> storage site (Sleipner area, North  
465 Sea). In: Baines, S. J. & Worden, R. H. (eds), Geological Storage of Carbon Dioxide.  
466 Geological Society Special Publication, 233, 165–180.

467 **Figures**

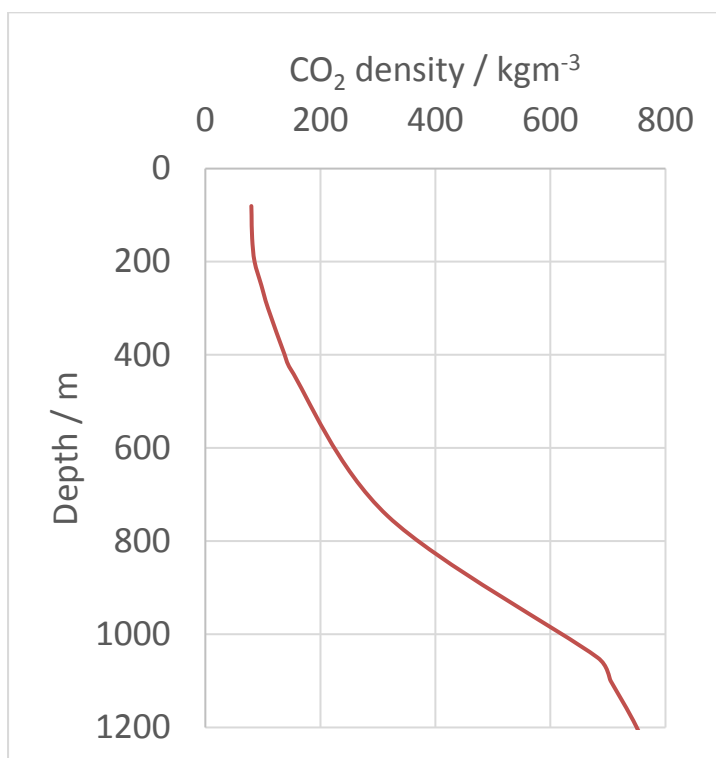


468

469 Figure 1: Cut-away view of the reservoir model for a non-leakage (left) and leakage scenario  
470 (right) for the 50m depth-to-crest model at 21 years, when the CO<sub>2</sub> first become detectable.  
471 CO<sub>2</sub> is multi-coloured with hot colours showing highest pore saturations, the vertical cross-  
472 sections show lithology, with grey shale and transparent sandstone.

473

474 Fig. 2 – Modelled CO<sub>2</sub> density with depth



475

Figure 3 – The change in gravity relative to the base case (zero injected CO<sub>2</sub>) for the 80 years of simulation for a no leakage scenario. See Fig. 1 for the location of the gravity survey stations. Note the slight asymmetry during injection, with a larger anomaly close to the injection well during injection.

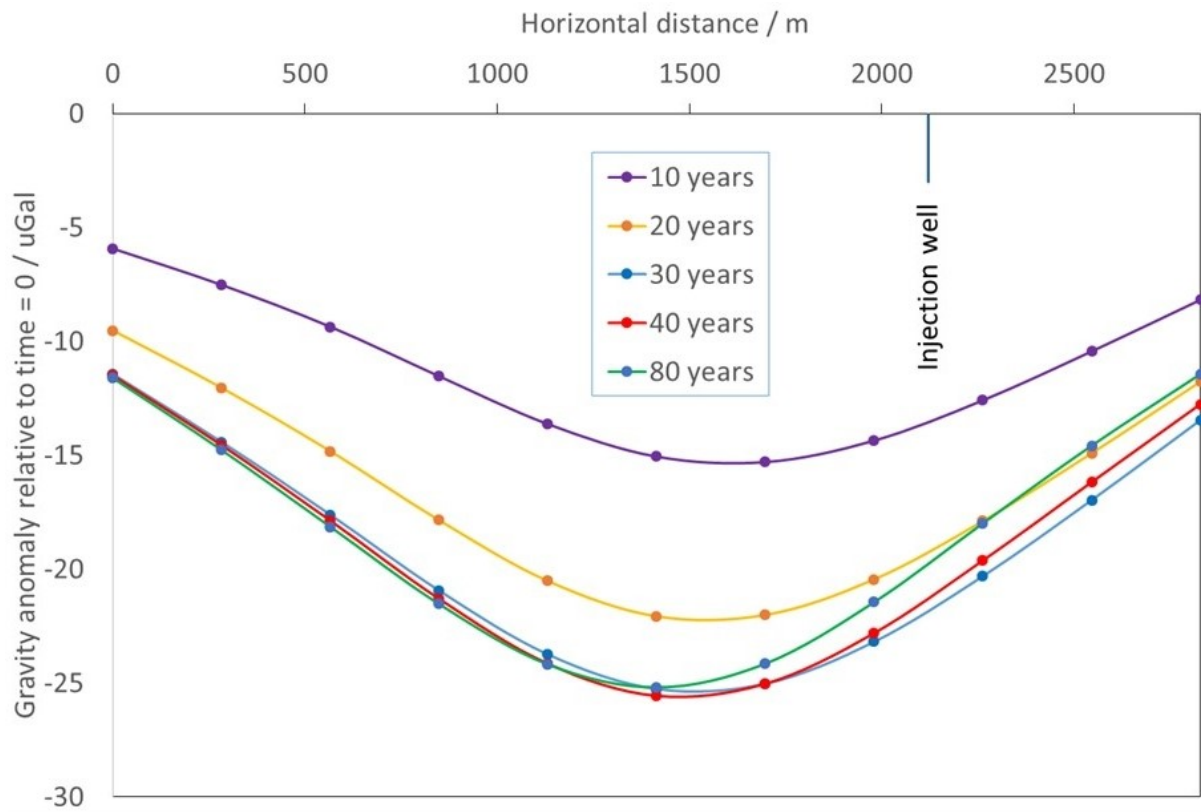


Figure 4 – Modelled gravity anomalies (relative to the no-leakage scenario) at 80 years after the start of injection, see Fig. 1 for the location of the survey stations. ‘Model X’ indicates an aquifer with a crestal depth of X m below the surface. The modelled anomalies are greater for the more shallow aquifers and are slightly asymmetric, being larger close to the leakage pathway, though this is not apparent on the figure.

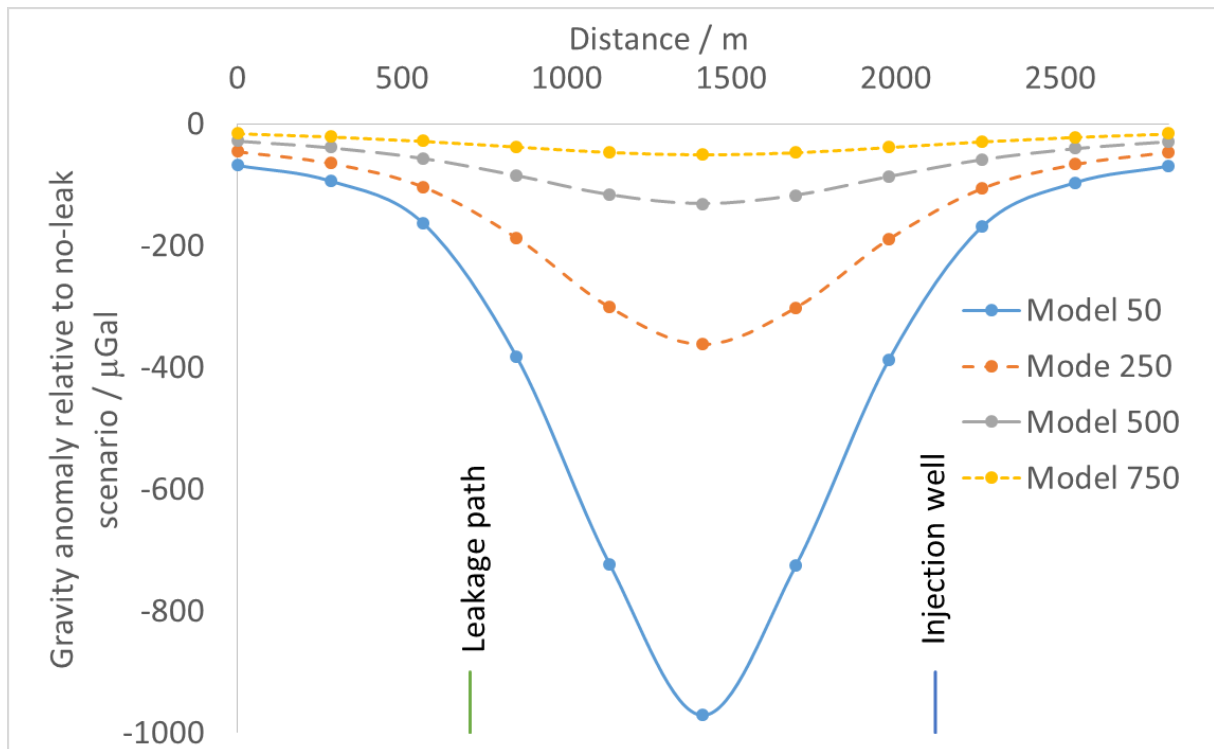
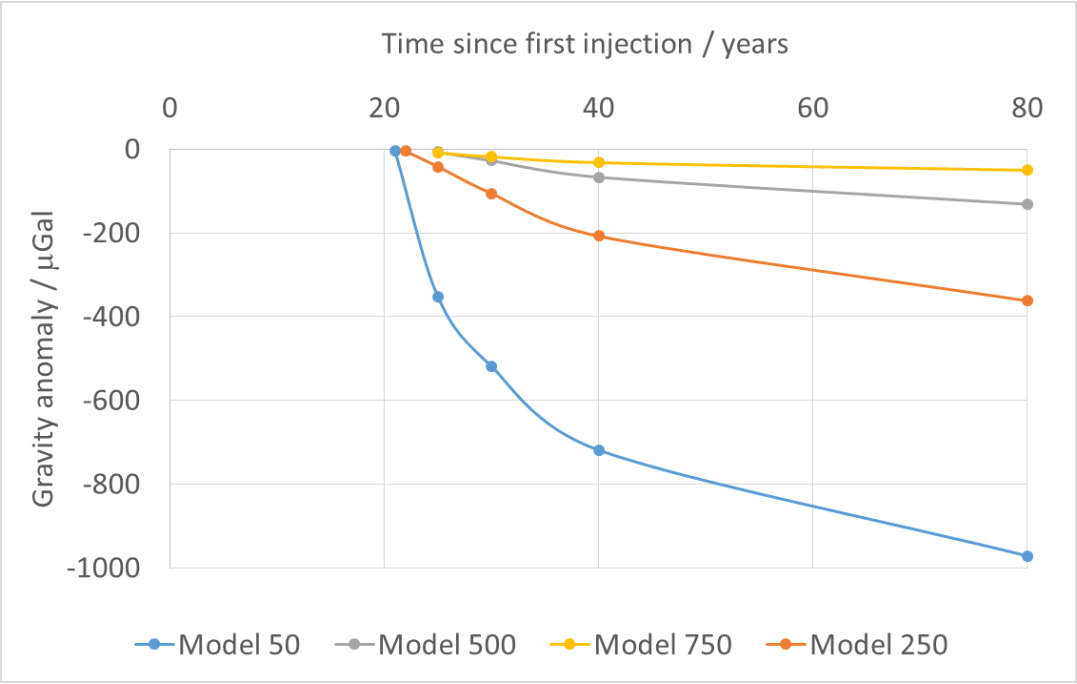


Figure 5 – Calculated maximum gravity anomaly (relative to the no-leakage scenario) through the 80 years of simulation of the 4 models, where ‘Model X’ indicates an aquifer with a crestal depth of X m below the surface



494 Table 1 – Summary of the geological model.

Parameter	Value
Model dimensions (horizontal)	2000 x 2000 m
Cell size	40 x 40 x 10 m (vertical)
Leakage pathway dimensions (horizontal)	40 x 40 m
Depth to crest of reservoir	1000 m
Thickness of reservoir	200 m
Depth to crest of aquifer	50 – 750 m
Thickness of aquifer	200 m
Reservoir geology	homogeneous
Reservoir and aquifer porosity	20 – 37 % (depth dependant)
Reservoir and aquifer permeability (horizontal)	30 – 200 mD
Reservoir and aquifer permeability (vertical)	0.1 x $K_{horizontal}$
CO <sub>2</sub> density	Duan & Sun (2003)
Relative permeability	Cardium Sandstone
Well location	Offset 500m x 500m from crest
Perforated interval	100m, top of reservoir

495

496 Table 2 – Gravity anomalies relative to the pre-injection ‘base case’ survey for a non-leakage  
497 scenario.

Time / Ma	Injected CO <sub>2</sub> / Mt	Calculated maximum gravity anomaly / $\mu$ Gal	Maximum anomaly ( $\mu$ Gal) / Mt CO <sub>2</sub> injected	Maximum anomaly ( $\mu$ Gal) / Mt CO <sub>2</sub> free-phase
0	0	0	-	-
10	10	-15.1	-1.5	-1.7
20	20	-22.0	-1.1	-1.3
30	30	-25.3	-0.84	-1.1
40	30	-25.6	-0.85	-1.2
80	30	-25.2	-0.84	-1.2

498

499



500 Table 3 - CO<sub>2</sub> parameters at first detection of leakage

501

Depth of top of aquifer / m	Detection time / years	Leakage time / Years	Mass injected / Mt	Mass of CO <sub>2</sub> in aquifer / Mt	% CO <sub>2</sub> in aquifer	Surface gravity anomaly / $\mu$ gal
50	21	15	21.3	0.006	0.03	-112
250	22	14	21.9	0.008	0.04	-5
500	25	14	25.0	0.07	0.3	-7
750	23	11	23.0	0.241	1.0	-6

502

503